Article

MRLIHT: Mobile RFID-Based Localization for Indoor Human Tracking

Qian Ma *, Xia Li, Guanyu Li, Bo Ning, Mei Bai and Xite Wang

College of Information Science and Technology, Dalian Maritime University, Dalian 116026, China;
lixia_email@163.com (X.L.); liguanyu@dlmu.edu.cn (G.L.); ningbo@dlmu.edu.cn (B.N.);
baimei@dlmu.edu.cn (M.B.); wangxite@dlmu.edu.cn (X.W.)
* Correspondence: maqian@dlmu.edu.cn; Tel.: +8613042456419

check for
updates

Abstract: Radio Frequency Identification (RFID) technology has been widely used in indoor location tracking, especially serving human beings, due to its advantage of low cost, non-contact communication, resistance to hostile environments and so forth. Over the years, many indoor location tracking methods have been proposed. However, tracking mobile RFID readers in real-time has been a daunting task, especially for achieving high localization accuracy. In this paper, we propose a new Mobile RFID (M-RFID)-based Localization approach for Indoor Human Tracking, named MRLIHT. Based on the M-RFID model where RFID readers are equipped on the moving objects (human beings) and RFID tags are fixed deployed in the monitoring area, MRLIHT implements the real-time indoor location tracking effectively and economically. First, based on the readings of multiple tags detected by an RFID reader simultaneously, MRLIHT generates the response regions of tags to the reader. Next, MRLIHT determines the potential location region of the reader where two algorithms are devised. Finally, MRLIHT estimates the location of the reader by dividing the potential location region of the reader into finer-grained grids. The experimental results demonstrate that the proposed MRLIHT performs well in both accuracy and scalability.

Keywords: RFID; mobile reader; fixed tag; indoor localization; human tracking

1. Introduction

Radio Frequency Identification (RFID) [1–3] is a technique of automatic identification using radio frequency transmission. RFID technology is widely used in many real-world applications, e.g., real-time tracking, activity recognition, etc, and impacts almost all aspects of people's daily life. An RFID system consists of readers and tags, where readers communicate with tags through radio signals. RFID tags are categorized as either active or passive. Active tags are powered by on-board batteries and broadcast their signals continuously, while passive tags are powered by the electromagnetic energy transmitted from RFID readers. Since the maturely developed GPS-based localization systems do not perform well for indoor location tracking applications, RFID-based localization technologies have become popular in several indoor tracking schemes. In this paper, we aim to propose an effective RFID-based localization approach for indoor human tracking, which can be pervasively used in the large-scale and high-accurate tracking applications.

Over the years, many RFID-based indoor human/object tracking methods have been proposed. They can be categorized as fixed RFID (F-RFID) model based and mobile RFID (M-RFID) model based tracking, whereas in the F-RFID (i.e., fixed RFID) model, RFID readers are pre-deployed at some fixed points in the monitoring area and RFID tags are attached on the moving objects, while in M-RFID (i.e., mobile RFID) model, RFID readers are equipped on the moving objects and RFID tags are fixed deployed at some points in the monitoring area. Generally, the two models are used for different

application scenarios. In large-scale monitoring applications, since the cost of RFID readers are very high, the deployment of fixed readers are generally sparse, which results that the location information of moving individuals (mobile tags) are discontinuous. In other words, there are phenomena of location information missing. To tackle this issue, some existing works estimate the missing location information based on the pre-defined motion model. Nevertheless, in most cases, the motion of individuals is arbitrary and cannot be predicted. On the other hand, to alleviate the sparseness of RFID readers, some existing works use the reference tags to instead replacing more readers. However, the localization accuracy is unsatisfactory (incurring meters of localization errors). In addition, to estimate the locations of moving human/objects based on the F-RFID model, the positions of fixed readers which are stored in the external storage medium (e.g., databases or files) are needed. The location information requirements incur extra query costs, and thereby reduces the tracking efficiency.

Therefore, in this paper, we propose a new Mobile RFID (M-RFID) based Localization approach for Indoor Human Tracking (MRLIHT). By deploying a large number of fixed and passive RFID tags in the monitoring area, the locations of moving individuals equipped with RFID readers are determined in real-time. The advantages that we adopt the M-RFID model and passive tags are as follows.

- Lower costs. Compared with active tags, the light-weight and small-volume passive tags without on-board batteries have longer lifetime and lower costs. Moreover, there is almost no maintenance cost [4]. On the other hand, in the scenario of human indoor location tracking, the RFID readers are held by human beings and can be reused many times, which are economical in a long-term perspective.
- Smaller localization errors. First, the sensing range of passive tags is smaller than that of active tags. During object localization, the candidate locations of an individual filtered by passive tags are more fine-grained, and thus the localization accuracy is improved. Second, by deploying passive tags intensively to cover the whole monitoring area, the location of a moving individual can be estimated continuously based on the location information of multiple tags received by the reader equipped on the moving object. Then the problem of location information missing introduced earlier can be effectively solved.
- Avoiding extra queries. With M-RFID model, RFID tags are fixed deployed in the monitoring area, rather than attaching on the moving individuals. Hence, the location information of passive tags can be written in their own memories and read by RFID readers directly. Therefore, the extra queries for location information are avoided.

For an individual, MRLIHT estimates its location by generating the response regions of tags detected by the reader attached to the individual first. Secondly, potential location region of the individual (reader) is determined based on those response regions. Finally, the final location of the individual is estimated with high accuracy and efficiency. The major contributions made in this paper are summarized as follows.

- We point out the pitfalls of existing works for large-scale and high-accurate tracking tasks. Accordingly, we develop an M-RFID based localization approach for indoor human tracking, named MRLIHT, to support high-quality moving humans tracking.
- By considering the influence of environmental noises, we extend the response region of an RFID tag to an RFID reader from a circle to a circular, which improves the localization accuracy.
- In MRLIHT, there is no pre-defined motion model for moving individuals, which are more suitable for real-world applications.
- For the fixed passive tags, the location information is written in their own memories directly. The RFID readers can obtain the location information of surrounding tags without extra query, which improves the location estimation efficiency.
- Finally, extensive experiments are conducted to evaluate the performance of the proposed approach.

The organization of the remaining paper is as follows. Section 2 discusses the related work. Section 3 presents the problem definition. Section 4 introduces the proposed MRLIHT system and Section 5 shows the experimental results. Finally, Section 6 concludes the paper.

2. Related Work

With the rapid development of big data [5], the idea of indoor location tracking based on RFID technology is widely used in many real applications. The traditional RFID-based indoor location tracking approaches can be classified into two classes: fixed RFID (F-RFID) based tracking and mobile RFID (M-RFID) based tracking.

Most of the existing works [6–8] are proposed for F-RFID model. In work [6], a localization framework, named LADNMARC, is proposed, where an indoor moving object is located based on the signal strengths received by nearby RFID readers. To improve the positioning accuracy while saving cost, LADNMARC proposes reference tags to instead replacing more readers. However, the deployment of RFID readers and reference tags are very strict in LADNMARC. RADAR [7] builds a signal propagation model by considering the impact of walls in indoor environments. It determines the location of an indoor object by combining the signal propagation model with empirical measurements. An indoor tracking method for navigating visually impaired people is proposed in [8]. The solution takes the signal strengths received by RFID readers as an observation vector, and determines the location of a user based on the Bayesian Decision Theory. The methods introduced above are active-tag-based systems, where the basic idea of location tracking is to make use of the signal strengths received by RFID readers and broadcast by active tags. However, since the sensing range of active tags is up to hundreds of meters, the localization error is large.

In addition, some works make use of passive tags to locate indoor objects based on the F-RFID model. PinIt [9] is a fine-grained RFID localization scheme proposed for nonline-of-sight scenarios. BackPos [10] is another fine-grained backscatter positioning technique based on the detected phase model. To reduce the labor and time cost of location fingerprinting, a cost-effective neighborhood graph-based localization system is proposed in [11]. However, all approaches mentioned above are mainly used for locating the static RFID tags and do not perform well in tracking the moving objects. In [12], an RFID data cleaning approach that supports location query is proposed. It estimates the location of moving objects based on Bayesian inference and taking advantage of duplicate readings. Since the Received Signal Strength Indicator (RSSI), which is widely adopted in active-tag-based tracking methods, is not available for passive tags, PassTrack [4] proposes a reader detection model based on the reading rates of passive tags. Then the location of a moving object is estimated based on the reader detection model. The work [13] studies the problem of cleaning RFID data streams for object tracking. To tracking objects in mobile environments, a probabilistic inference model is proposed. However, all the passive-tag-based indoor tracking algorithms introduced above need to be assigned a motion model to moving objects. In practice, the movement of indoor objects are generally arbitrary and unpredictable. OTrack [14] is proposed to track the luggage attached with tags in the airport based on the temporal correlation among the communications between the RFID readers and tags. However, such a scheme usually requires specific application scenarios. Tagoram [15] achieves the goal of tracking mobile RFID tags in real-time by leveraging the phase value of the backscattered signal, which suffering the problem of multipath reflections. MobiTagbot [16] constructs a holography to locate RFID tags using antenna movements and frequency hopping. However, MobiTagbot is time-consuming for large-scale monitoring areas and impractical for real-time localization.

By comparison, the M-RFID based indoor tracking method is few. In [17], the authors propose to use relatively fixed tags to locate a moving human/object with a mobile reader. Considering the location uncertainty of the moving objects, the work proposes a probabilistic model to locate the moving objects. However, the algorithm is also based on the assumption that the motion model of moving objects is known, which limits its applications. In work [18], the proposed data cleaning approach for mobile RFID data streams is capable of large tracking and monitoring environments.

The rationale of the proposed approach is similar to those methods based on the F-RFID model and only considers the case of a single reader. The works [19,20] use the memory of passive tags to encode and store the information of moving objects. Then the proposed algorithms estimate the locations of moving objects through creating an information-gradience. However, the approaches are time-consuming and not capable of real-time localization. In work [21], a phase-based localization algorithm is proposed to locate a device moving equipped with a UHF RFID reader.UHF (Ultra High Frequency) RFID reader is a kind of RFID reader where the frequency range is from 300 MHz to 1 GHzIn this work, the mobile device is supposed to move along a known path (e.g., x-coordinate) and its location at an assigned temporal can be estimated by using the phase differences between the RFID reader and reference tags besides the path. Moreover, the moving speed of the mobile device and its location on other coordinates (e.g., y-coordinate and z-coordinate) are also needed, which is difficult to obtain in practice. Some works, e.g., STPP [22] and TagSort [23] propose the concept of relative localization. They determine the order (or relative location) of fixed tags by exploring the change of phase information of tags when a moving reader approaches or moves away. However, the proposed methods focus on obtaining the order of tags rather than the absolute location of tags. Moreover, they are proposed for positioning the static objects which are not competent for the moving objects. On the other hand, there are some works are suitable for both F-RFID and M-RFID, e.g., *k*-nearest-neighbor-based localization [24,25] and multilateration-based localization [26], but their localization accuracy are needed to be improved. In this paper, we propose a new approach based on the M-RFID model to tracking indoor humans with high-accuracy and in real-time.

3. Problem Statement

Suppose there are n RFID tags $\mathcal{T} = \{T_1, T_2, \cdots, T_n\}$ and m RFID readers $\mathcal{R} = \{R_1, R_2, \cdots, R_m\}$ in the monitoring area, where the RFID tags are deployed at some fixed points and RFID readers are handheld or equipped on the moving individuals. The main goal of this work is to determine the locations of moving individuals in real-time. In the following, we first formally define some terms used throughout the paper.

Definition 1. *A reading, denoted by $D = (Rid, Tid, Tloc, Time, Count)$, is a data tuple with information of an RFID tag by an RFID reader, where Rid and Tid are the unique identifications of the reader and tag respectively, Tloc is the location of the tag, Time is a unit time point and Count is the number of times the tag detected by the reader in unit time.*

In this paper, we use 2D coordinate to denote the location of an RFID tag (or an RFID reader), i.e., the location of an RFID tag T_j (or an RFID reader R_i) can be denoted by $T_j.loc = (T_j.X, T_j.Y)$ (or $R_i.loc = (R_i.X, R_i.Y)$). Moreover, it is notable that, in the F-RFID model, the reading of a tag by a reader is usually denoted by a triple $(Rid, Tid, Time)$ without the information about tag location and the number of detection times. It is because, with the F-RFID model, RFID tags dynamically move with the moving objects (human beings), while the memories of RFID tags are limited and unavailable for being written frequently. By comparison, in M-RFID model, the RFID tags are fixed and thus their locations can be written into their own memories once only. In addition, since RFID readings are of low quality, the read frequency of RFID readers is high. Hence, an RFID tag can be detected multiple times by an RFID reader in unit time. To save storage space and reduce the data complexity, we aggregate multiple readings of a tag by an RFID reader in unit time into a single reading by adding the *Count* attribute (as introduced in Definition 1).

Example 1. *Figure 1 is the plan of a large-scale indoor exhibition area where many spots can be visited. To tracking visitors accurately, a large number of RFID passive tags are intensively deployed in the monitoring area (denoted by the red circle in the figure) and RFID readers are equipped on the moving objects (i.e., the visitors). Note that with the development of hardware, the portable and small RFID reader has been widely used*

in many real applications. Specifically, the distribution of tags detected by reader R_3 at time t_1 is shown in the right subfigure where ten tags, i.e., $T_1 \sim T_{10}$, are detected by R_3 simultaneously. Suppose the reading of a tag (e.g., T_4) by reader R_3 at time t_1 is $D_{3,4} = (R_3, T_4, (2,8), t_1, 7)$. It means that at time t_1, tag T_4 is detected seven times by reader R_3.
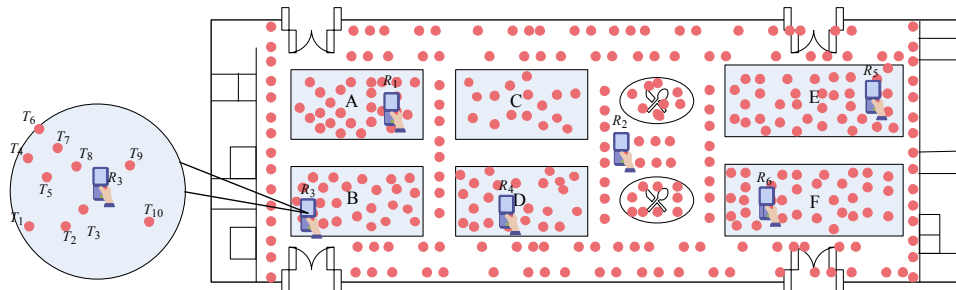
Figure 1. The plan of a large-scale indoor exhibition area.

As introduced earlier, the passive RFID tags are powered by the energy from RFID readers instead of on-board batteries. An RFID reader emits an electromagnetic energy field of a few feet, and any RFID tag in the vicinity may receive the energy and response its information.

Definition 2. *With the M-RFID model, when a fixed tag responds to a moving reader, the region where the reader may locate in is the Response Region (RR) of the tag to the reader.*

Moreover, a reader may detect multiple tags simultaneously due to the intensive deployment of tags and large sensing range of the reader.

Definition 3. *The Potential Location Region (PLR) of a reader is the overlap region of tag response regions which are generated by the tags detected by the reader simultaneously.*

On the other hand, even though an RFID tag locates in the sensing range of an RFID reader, it may not respond to the reader successfully, as the energy gathered by the tag may not enough to respond. In other words, an RFID tag is detected by an RFID reader with a certain probability, rather than definitive.

Definition 4. *The reading rate of an RFID tag by an RFID reader, denoted by τ, is the probability of the tag is detected by the reader.*

Since the Received Signal Strengths Indicator (RSSI) measurement which usually adopted in active-tag-based systems, is not available for passive tags, we aim to leverage the reading rate to obtain the location information of moving objects (persons). To achieve this goal, we propose an M-RFID based Indoor Location Tracking (MRLIHT) system. At time *t*, given the readings of tags by each reader, MRLIHT aims to tackle the following issues:

- Generating the response region of each tag detected by a reader simultaneously.
- Determining the potential location region (PLR) for each RFID reader.
- Estimating the location of each RFID reader (i.e., moving object) precisely.

Finally, the locations of moving persons at each time point are returned with high-accuracy and in real-time.

4. MRLIHT System

In this section, we introduce the proposed MRLIHT which consists of three components: RR generation, PLR determination and location estimation to tackle the issues mentioned above.

4.1. RR Generation

As introduced earlier, we use the reading rate of a passive tag by a reader to determine the location of an indoor moving individual. Specifically, there are two ways to estimate the reading rate.

One way is to use the response count in a fixed number of interrogation cycles sent from the reader. In this work, we estimate the reading rate of a tag T_i by a reader R_i as

$$\tau_{ij} = \frac{Count_{ij}}{C_i}, \tag{1}$$

where $Count_{ij}$ is the number of times tag T_j detected by reader R_i and C_i is the total number of interrogation times of reader R_i in unit time. For example, if a reader receives responses from a tag in 30 out of 100 interrogation times in unit time (e.g., 1 second), then the reading rate of the tag by the reader is 0.3.

Another way is to estimate the reading rate of a tag by a reader based on the reader detection model, where the reading rate is estimated by a function about the distance between the tag and the reader. In this work, we adopt the Sigmoid model to quantify the reading rate with distance proposed in [4], because the reader detection model is more accurate than the traditional 3-state model [12]. For an RFID tag T_j, the reading rate of T_j by an RFID reader R_i is shown below

$$\tau_{ij}\left(l_{ij}\right) = \frac{1}{1 + e^{a_i l_{ij} + b_i}}, \ (a_i > 0, b_i > 0). \tag{2}$$

In Equation (2), a_i and b_i are the parameters of reader R_i and can be learned from the readings of the detected tags by the reader R_i. The variate l_{ij} is the distance between the reader R_i and tag T_j. Since the reading rate of tag T_j by reader R_i can be obtained through the readings of T_j by R_i based on Equation (1), the distance l_{ij} between R_i and T_j in Equation (2) can be computed below

$$l_{ij} = \frac{1}{a_i}\left[ln\left(\frac{1}{\tau_{ij}} - 1\right) - b_i\right]. \tag{3}$$

As introduced earlier, the locations of readers and tags are denoted by the points with 2D coordinate. The Euclidean distance between R_i and T_j is $l_{ij} = \sqrt{\left(R_i.X - T_j.X\right)^2 + \left(R_i.Y - T_j.Y\right)^2}$. Then we have

$$\left(R_i.X - T_j.X\right)^2 + \left(R_i.Y - T_j.Y\right)^2 = l_{ij}^2, \tag{4}$$

where l_{ij} can be computed based on Equation (3), the location of tag T_j, i.e., $T_j.loc = (T_j.X, T_j.Y)$ is known and the location of reader R_i, i.e., $R_i.loc = (R_i.X, R_i.Y)$ is the goal we aim to determine. From Equation (4), we can know that the region where reader R_i may locate in, i.e., the response region (RR) of tag T_j to reader R_i, is the circle with center $(T_j.X, T_j.Y)$ and radius l_{ij}.

In addition, due to the influence of environmental noises and the antenna direction settings of the reader, the reading rate of a tag by a reader has certain errors. Based on the theory of radio propagation, for the same source (i.e., reader), the error of signal strength (denoted by ϵ) received by various receivers (i.e., tags) follow the same statistical law, i.e., the Gaussian error model $\varepsilon \sim N\left(\mu, \sigma^2\right)$ [27]. Therefore, in this paper, we suppose that the error of R_i's reading rate follows the Gaussian distribution with mean 0 and variance σ_i^2, i.e., $\varepsilon_i \sim N\left(0, \sigma_i^2\right)$, where the mean is 0 as we believe that the methods do not make errors on purpose and the variance σ_i^2 can be estimated based on the readings of the tags by the reader. Therefore, given a confidence value $1 - \alpha$, we have

$$p\left(-N\left(1-\alpha/2\right) < \left|\frac{\varepsilon_i}{\sigma_i}\right| < N\left(1-\alpha/2\right)\right) = 1 - \alpha.$$

Adding the error ε_i on the reading rate τ_{ij}, the range of reading rate of tag T_j by reader R_i is

$$\left(\tau_{ij} - \sigma_i N\left(1-\alpha/2\right), \tau_{ij} + \sigma_i N\left(1-\alpha/2\right)\right). \tag{5}$$

Combining Equation (5) with Equation (3), the range of distance between reader R_i and tag T_j is $l_i \in [l_{min}, l_{max}]$, where

$$l_{min} = \frac{1}{a_i}\left[ln\left(\frac{1}{\tau_{ij} + \sigma_i N\left(1-\alpha/2\right)} - 1\right) - b_i\right],$$

$$l_{max} = \frac{1}{a_i}\left[ln\left(\frac{1}{\tau_{ij} - \sigma_i N\left(1-\alpha/2\right)} - 1\right) - b_i\right].$$

Finally, the response region (RR) of tag T_j to reader R_i becomes a circular region with center $\left(T_j.X, T_j.Y\right)$ and radius l_{min} and l_{max}.

Example 2. *For the reader R_3 and tag T_4 mentioned in Example 1, suppose the reading rate of T_4 by R_3 is $\tau_{3,4} = 0.8$, the variance σ_3 of error ϵ_3 is $\sigma_3 = 0.1$ and the confidence value is $1 - \alpha = 0.9$. Moreover, let the parameters of reader detection model are $a_3 = 9,843$ and $b_3 = -16.2015$. We can compute that $l_{min} = 1.379$ and $l_{max} = 1.584$. Then the response region of tag T_4 to reader R_3 is shown in Figure 2a.*

(a)　　　　　　　　　　　　(b)
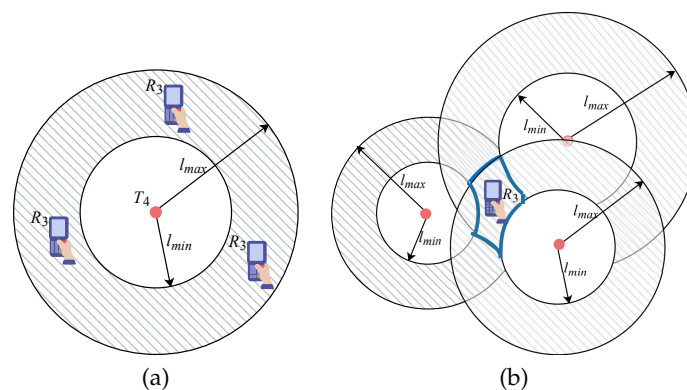
Figure 2. (**a**) The response region of tag T_4 to reader R_3 and (**b**) the Potential Location Region (PLR) of reader R_3.

4.2. PLR Generation

Thus far, given an RFID reader R_i and an RFID tag T_j detected by R_i, we can obtain the RR (response region) of T_j to R_i. Next, we aim to determine the potential location region (PLR) of a reader by employing the RRs of tags detected by the reader simultaneously.

4.2.1. Exact Solution

Based on Definition 3, the PLR (potential location region) of R_i is derived by taking the overlap of RRs of multiple tags detected by R_i simultaneously.

Example 3. *(Example 2 Continued) The PLR of reader R_3 derived by the RRs of three tags it detected simultaneously is shown in Figure 2b (the polygon surrounded by the blue curve). Since it is difficult to show the intersection of RRs of ten tags detected by reader R_3 simultaneously, we only show the PLR of R_3*

derived by RRs of three tags it detected simultaneously. Moreover, Note that in practice, a reader may detect a large number of tags simultaneously due to the intensive deployment of passive tags.

Algorithm 1 shows the pseudo-code of the exact solution of PLR (potential location region) generation. As shown, for each reader R_i, we need to compute the RR (response region) of each tag T_j detected by R_i simultaneously, and taking the overlap of multiple RRs to generate the PLR of R_i. Since a tag may also be detected by multiple readers, the time complexity of the exact PLR generation solution is $O(mn)$ where m and n are the numbers of readers and tags in the monitoring area, respectively.

Algorithm 1: PLRGenExact($\mathcal{T}$, $\mathcal{R}$, $\mathcal{D}$, a_i, b_i, α).

Input : The tag set $\mathcal{T} = \{T_1, T_2, \cdots, T_n\}$, the reader set $\mathcal{R} = \{R_1, R_2, \cdots, R_m\}$, the reading
set $\mathcal{D}$, and parameters a_i, b_i and α
Output: The *PLR* of each reader

1 **foreach** *Reader $R_i \in \mathcal{R}$* **do**
2     $PLR_i = W$ //W indicates the whole monitoring region
3   **foreach** *Tag T_j detected by R_i* **do**
4   // computing the reading rate of T_j by R_i based on Equation (1)
5        $\tau_{ij} = \frac{Count_{ij}}{C_i}$
6   // computing l_{min} and l_{max}
7        $l_{min} = \frac{1}{a_i}\left[ln\left(\frac{1}{\tau_{ij}+\sigma_i N(1-\alpha/2)} - 1 \right) - b_i \right]$
8        $l_{max} = \frac{1}{a_i}\left[ln\left(\frac{1}{\tau_{ij}-\sigma_i N(1-\alpha/2)} - 1 \right) - b_i \right]$
9   //generating the RR of T_j by R_i
10       $RR_i = Circular(T_j.loc, [l_{min}, l_{max}])$
11   // the PLR of reader R_i is the overlap of multiple tags detected by R_i
12       $PLR_i = PLR_i \bigcap RR_i$

13 **return** PLR_i

4.2.2. Approximate Solution

The exact solution may be inefficient for large-scale tracking applications where there are hundreds of thousands or millions of passive tags deployed in the monitoring area. Under this scenario, a large number (dozens or even hundreds) of tags may be detected by a reader simultaneously. As a result, the time complexity of *PLR* generation is extremely high by taking the overlap of multiple detected tags. Moreover, due to the intensive deployment, some RFID tags are close to each other, which results that the RRs of these tags are almost the same. To avoid redundant computation, we further propose an approximate solution to generate the *PLR* for each reader. The approximate solution consists of two steps: (1) tag group generation and (2) *PLR* determination. Next, we introduce each step in detail.

First, we divide the RFID tags into tag groups defined below.

Definition 5. *Tag Group. A tag group G contains a collection of tags satisfying that*

(i) $\forall T_j \in G, \exists T_k \in G, d(T_j, T_k) \leq \delta_d$ *where $d(T_j, T_k)$ is the distance between T_j and T_k and δ_d is the distance threshold.*

(ii) $|G| \geq \delta_s$ *where $|G|$ is the size of the tag group, i.e., the number of tags contained in G, and δ_s is the size threshold.*

Note that we use the distance threshold δ_d to control the extension ability of a tag group, i.e., more tags may be included in a tag group with a greater δ_d. On the other hand, we use the size threshold δ_s

to avoid that sparse tags which have big distance are included into a tag group under the scenario of great δ_d.

Algorithm 2 shows the pseudo-code of the tag group generation, where the specific steps are as follows:

(s1) Initializing a candidate tag group G and generating a seed list (denoted by $\mathcal{S}$) which is the copy of tag set $\mathcal{T}$ (Line2-3).

(s2) Selecting a tag T_j randomly as seed and removing it from the seed list $\mathcal{S}$ (Lines 5 and 6).

(s3) Computing the distance between each tag $T_k \in \mathcal{T}$ and the seed T_j (Line 9). Adding T_k into the candidate tag group G and removing T_k from the tag set $\mathcal{T}$, if the distance is smaller than the given distance threshold δ_d. Otherwise, removing T_k from the seed list $\mathcal{S}$ (Line 10-14).

(s4) Repeating steps (s2) and (s3) until the seed list is empty, which means the distances between the remaining tags in the tag set and any tag in the candidate tag group G are greater than δ_d.

(s5) Adding the candidate tag group into the set of tag groups $\mathcal{G}$ (Line 15).

(s6) Repeating steps (s1)–(s5) until the tag set is empty, i.e., all tags are classified into a certain tag group.

(s7) Determining each size of the candidate tag group. If the size is greater than the give size threshold δ_s, it is a real tag group. Otherwise, remove the candidate tag group from $\mathcal{S}$ (Line 16–18). Finally, returning the set of tag group $\mathcal{G}$.

Algorithm 2: TagGroupGen($\mathcal{T}$, δ_d, δ_s).

Input : The tag set $\mathcal{T} = \{T_1, T_2, \cdots, T_n\}$, the distance threshold δ_d and the size threshold δ_s
Output: The collection of tag groups $\mathcal{G} = \{G_1, G_2, \cdots, G_{n'}\}$

1 **while** $\mathcal{T}$ *is not empty* **do**
2    $G = \Phi$ //initial a candidate tag group
3    $\mathcal{S} = \mathcal{T} = \{T_1, T_2, \cdots, T_n\}$ //a copy of tag set
4   **while** $\mathcal{S}$ *is not empty* **do**
5      $T_j = RandomSelect(\mathcal{S})$ //randomly select a tag from $\mathcal{S}$
6      $\mathcal{S}.remove(T_j)$
7   **foreach** $T_k \in \mathcal{T}$ **do**
8   //compute the distance between tag T_j and T_k
9        $d\left(T_j, T_k\right) = \sqrt{\left(T_j.X - T_k.X\right)^2 + \left(T_j.Y - T_k.Y\right)^2}$
10   **if** $d\left(T_j, T_k\right) \leq \delta_d$ **then**
11          $G.add(T_k)$
12          $\mathcal{T}.remove(T_k)$
13   **else**
14          $\mathcal{S}.remove(T_k)$
15    $\mathcal{G}.add(G)$
16 **foreach** $G \in \mathcal{G}$ **do**
17   **if** $|G| < \delta_s$ **then**
18 $\mathcal{G}.remove(G)$
19 **return** $\mathcal{G}$

The time complexity of tag group generation is $O\left(n^2\right)$ and $O\left(n\right)$ in the worst case where each tag is considered as a tag group and in the best case where all RFID tags are considered as a tag group, respectively. Thus the average time complexity of tag group generation is $O\left(nlogn\right)$. Moreover, since our work is proposed based on the M-RFID model where RFID tags are fixed deployed in the monitoring area, the tag group generation only needs to conduct one time. On the other hand, it is notable that an RFID tag may not belong to any tag group. For such tags, they are considered independent and used to *PLR* determination with aggregated tags (to be introduced later) together.

After dividing tags into tag groups, we use the aggregated tags (generated based on the tag groups) to determine the *PLR* for each reader.

Definition 6. *Aggregated Tag. For a tag group G, the aggregated tag T_a is the representation of G. Moreover, the reading of T_a by a reader R_i at a certain time point is computed based on the readings of tags by R_i.*

Given an RFID reader R_i, suppose the tag set detected by R_i simultaneously (i.e., at a certain time point t), is $\mathcal{T}_i = \{T_1, T_2, \cdots, T_q\}$. We first determine each tag $T_j \in \mathcal{T}_i$ belonging to which tag group. Then we generate the aggregate tags of corresponding tag groups used for R_i's *PLR* generation. Since RFID tags are fixed, it is easy to locate tag $T_j \in \mathcal{T}_i$ belongs to which tag group by building an inverted index. Specifically, during the tag group generation, we build an inverted index for each tag T_j to record the tag belongs to which tag group. The structure of the inverted index is shown in Figure 3. Note that as mentioned earlier, an RFID tag may not belong to any tag group. Accordingly, in the inverted index, the tag points to 'Null' if it does not belongs to a tag group. Next, we introduce how to generate an aggregate tag for each tag group used for R_i's *PLR* generation.
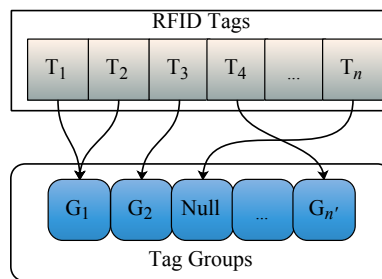
Figure 3. The structure of the inverted index for Radio Frequency Identification (RFID) tags.

Suppose the tags detected by R_i simultaneously belongs to w tag groups $\mathcal{G}_i = \{G_1, G_2, \cdots G_w\}$ where $G_k = \{T_{k,1}, T_{k,2}, \cdots, T_{k,q'}\}$ ($T_{k,j} \in \mathcal{T}_i$ and $q' \leq q$) and the reading of $T_{k,j}$ by R_i is $D_{k,j} = \left(Rid_{k,j}, Tid_{k,j}, Tloc_{k,j}, Time_{k,j}, Count_{k,j}\right)$. We aim to obtain the reading of the aggregated tag corresponding to the tag group $G_k \in \mathcal{G}_i$, denoted by $T_{a,k} = (Rid_{a,k}, Tid_{a,k}, Tloc_{a,k}, Time_{a,k}, Count_{a,k})$.

Since any tag $T_i \in \mathcal{T}_i$ is detected by reader R_i at a certain time point t, we have $Rid_{a,k} = R_i$, $Time_{a,k} = t$. In addition, we assign a unique ID for $T_{a,k}$ based on an independent number system. Next, we need to determine the location of the aggregated tag $Tloc_{a,k}$ and the number of detection times $Count_{a,k}$. In real applications, the distance between an RFID tag T_j and a reader R_i is smaller, the reading rate of T_j by R_i is higher, and thereby the location of the T_j (used for determining the location of R_i) is more important. Therefore, we compute $Tloc_{a,k}$ and $Count_{a,k}$ by the weighted average of corresponding information of various tags, as shown below.

$$Tloc_{a,k}.X = \frac{\sum w_{k,j} \times T_{k,j}.X}{\sum w_{k,j}} \tag{6}$$

$$Tloc_{a,k}.Y = \frac{\sum w_{k,j} \times T_{k,j}.Y}{\sum w_{k,j}} \tag{7}$$

$$Count_{a,k} = \frac{\sum w_{k,j} \times Count_{k,j}}{\sum w_{k,j}} \tag{8}$$

$$w_{k,j} = \frac{Count_{k,j}}{\sum Cout_{k,j}} \tag{9}$$

The pseudo-code of aggregated tag generation is shown in Algorithm 3.

**Algorithm 3:** AggregatedTagGen(R_i, $\mathcal{T}_i$)

   Input : A reader R_i, the tag set $\mathcal{T}_i = \{T_1, T_2, \cdots, T_q\}$ detected by R_i simultaneously, the tag groups $\mathcal{G}$

   Output: The aggregated tags $\{T_{a,1}, T_{a,2}, \cdots, T_{a,q'}\}$

1 //the set of tag group of each $T_j \in \mathcal{T}_i$ belongs to
2 $\mathcal{G}_i = \Phi$
3 **foreach** *Tag $T_j \in \mathcal{T}_i$* **do**
4   **if** *T_j points to tag group G_k in the inverted index* **then**
5   G_k.add(T_j)
6         $\mathcal{G}_i$.add(G_k)

7 **foreach** *Tag group $G_k \in \mathcal{G}_i$* **do**
8   //generate the reading of aggregated tag corresponding to G_k
9     $T_{a,k} = (Rid_{a,k}, Tid_{a,k}, Tloc_{a,k}, Time_{a,k}, Count_{a,k})$
10     $Tloc_{a,k}.X = \frac{\sum w_{k,j} \times T_{k,j}.X}{\sum w_{k,j}}$
11     $Tloc_{a,k}.Y = \frac{\sum w_{k,j} \times T_{k,j}.Y}{\sum w_{k,j}}$
12     $Count_{a,k} = \frac{\sum w_{k,j} \times Count_{k,j}}{\sum w_{k,j}}$
13     $w_{k,j} = \frac{Count_{k,j}}{\sum Cout_{k,j}}$

14 **return** $\{T_{a,k}\}$

Example 4. *(Example 1 Continued) We map the distribution of ten tags detected by R_3 simultaneously at time t_1 into a 2D coordinate system, as shown in Figure 4a. Additionally, the readings of tags by R_3 is shown in Table 1. The tag groups generated based on Algorithm 2 with $\delta_d = 35$ cm and $\delta_s = 3$ is shown in Figure 4b. Note that the candidate tag group G_3 is removed since its size is smaller than the threshold δ_s. Finally, based on Algorithm 3, the readings of corresponding aggregated tags are shown in Table 2.*

| | (a) | | (b) |
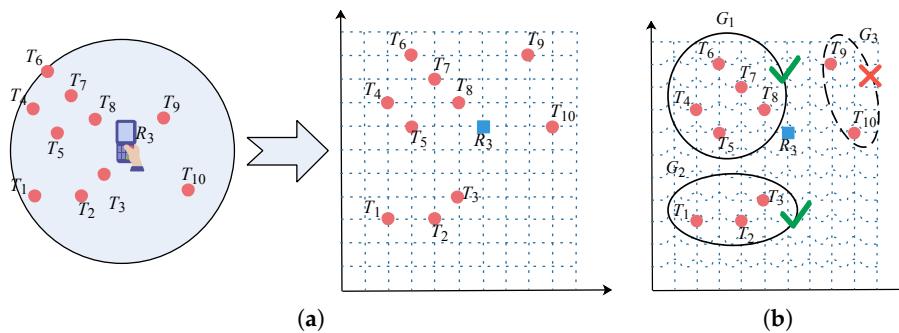
Figure 4. (**a**) Distribution of tags detected by R_3 and (**b**) readings of tags by reader R_3.

Table 1. Readings of tags by reader R_3.

Observations	
$(R_3, T_1, (2,3), t_1, 5)$	$(R_3, T_6, (3,10), t_1, 6)$
$(R_3, T_2, (4,3), t_1, 6)$	$(R_3, T_7, (4,9), t_1, 10)$
$(R_3, T_3, (5,4), t_1, 9)$	$(R_3, T_8, (5,8), t_1, 20)$
$(R_3, T_4, (2,8), t_1, 7)$	$(R_3, T_9, (8,10), t_1, 8)$
$(R_3, T_5, (3,7), t_1, 9)$	$(R_3, T_{10}, (9,7), t_1, 9)$

Table 2. Readings of aggregated tags by reader R_3.

Observations
$(R_3, T_{a,1}, (3.95, 3.25), t_1, 7)$
$(R_3, T_{a,2}, (3.83, 8.25), t_1, 13)$

After aggregated tag generation, we can determine the *PLR* for each reader based on the aggregated tags. The pseudo-code is shown in Algorithm 4, where for each reader $R_i \in \mathcal{R}$, we first generate the readings of aggregated tags based on the readings of tags detected by R_i simultaneously (Line 3). Note that the tags which do not belong to any tag group are also used for PLR determination. Thus the tag list $\mathcal{T}'$ is generated by combining such independent tags and aggregated tags together to determine the PLR of R_i (Line 5). Afterwards, the PLR of R_i is determined by intersecting the RR of each tag in the tag list $\mathcal{T}'$, where the procedure is the same as the exact solution (Line 7-16). Suppose n tags are divided into n' tag groups. Then the time complexity of approximate solution becomes $O(mn')$ which is much smaller than the exact solution since $n' \ll n$. Note that the computational cost of tag group generation is not included since it can be pre-computed once the tag deployment finished.

Algorithm 4: PLRGenApproximate($\mathcal{T}, \mathcal{R}, \mathcal{D}, a_i, b_i, \alpha$)

Input : The tag set $\mathcal{T} = \{T_1, T_2, \cdots, T_n\}$, the reader set $\mathcal{R} = \{R_1, R_2, \cdots, R_m\}$ and the reading set $\mathcal{D}$

Output: The *PLR* of each reader

1 **foreach** *Reader $R_i \in \mathcal{R}$* **do**
2 　 //generate the aggregated tags
3 　 $\left\{ T_{a,1}, T_{a,2}, \cdots, T_{a,q'} \right\} = \textbf{AggregatedTagGen}(R_i, \mathcal{T}_i)$
4 　 //Combining the aggregated tags and the independent tags which do not belong to any tag group
5 　 $\mathcal{T}_i' = \left\{ T_{a,1}, T_{a,2}, \cdots, T_{a,q'}, T_1, T_2, \cdots, T_{q''} \right\}$
6 　 $PLR_i = W$ //W indicates the whole monitoring region
7 　 **foreach** *Tag $T_j \in \mathcal{T}_i'$* **do**
8 　　 // computing the reading rate of T_j by R_i based on the readings of R_i and Equation (1)
9 　　 $\tau_{ij} = \frac{Count_{ij}}{C_i}$
10 　　 // computing l_{min} and l_{max}
11 　　 $l_{min} = \frac{1}{a_i} \left[ln \left(\frac{1}{\tau_{ij} + \sigma_i N(1 - \alpha/2)} - 1 \right) - b_i \right]$
12 　　 $l_{max} = \frac{1}{a_i} \left[ln \left(\frac{1}{\tau_{ij} - \sigma_i N(1 - \alpha/2)} - 1 \right) - b_i \right]$
13 　　 //generating the RR of T_j by R_i
14 　　 $RR_i = Circular(T_j.loc, [l_{min}, l_{max}])$
15 　　 // the PLR of reader R_i is the overlap of multiple tags detected by R_i
16 　　 $PLR_i = PLR_i \bigcap RR_i$
17 **return** PLR_i

4.3. Location Estimation

Thus far, for each reader, we get its possible locations. In this section, we aim to estimate the precise location for each reader.

We propose a location estimation algorithm based on the grid. Given a reader R_i which detects q tags, i.e., $\mathcal{T}_i = (T_1, T_2, \cdots, T_q)$, at a certain time point t, we first divide its PLR into grids where the grid granularity can be specified by users. Then each grid is considered as a location and denoted by its center point. Next, for each grid g_k, we compute the Root Mean Square Error (RMSE) of the reading

rate of tags detected by R_i simultaneously, by supposing that reader R_i locates at g_k. Specifically, the RMSE of reading rate is denoted by $s_k = \sqrt{\frac{1}{q} \sum_{T_j \in \mathcal{T}_i} \left(\tau'_{ij} - \tau_{ij} \right)^2}$, where τ'_{ij} and τ_{ij} are the reading rates computed based on Equations (1) and (2) respectively. Finally, we select the grid where the RMSE of reading rate is the smallest as the precise location of reader R_i, because a smaller RMSE means that the grid is closer to the real location of the reader. The pseudo-code of the algorithm is shown in Algorithm 5.

Algorithm 5: LocationEstimation($\mathcal{R}$, $\{PLR_i\}$)

> **Input** : The reader set $\mathcal{R} = \{R_1, R_2, \cdots, R_m\}$, the PLR of each reader PLR_i
> **Output**: The precise location of each reader, i.e., $R_i.loc$

1 **foreach** *Reader $R_i \in \mathcal{R}$* **do**
2   //divide the PLR of R_i into grids
3     $\mathbf{g} = \{g_1, g_2, \cdots\}$
4     $s_{kmin} = \infty$
5   **foreach** *grid $g_k \in \mathbf{g}$* **do**
6   //compute the RMSE of reading rate of tags detected by reader R_i simultaneously
7         $s_k = 0$
8   **foreach** *tag $T_j \in \mathcal{T}_i$* **do**
9             $\tau'_{ij} = \frac{Count_{ij}}{C_i}$
10             $\tau_{ij} = \frac{1}{1 + e^{a_i l_{ij} + b_i}}$, $(a_i > 0, b_i > 0)$
11             $s_k = s_k + \left(\tau'_{ij} - \tau_{ij} \right)^2$
12         $s_k = \sqrt{\frac{s_k}{q}}$
13   **if** *$s_k < s_{kmin}$* **then**
14             $R_i.loc = g_k$
15             $s_{kmin} = s_k$

16 **return** $\{R_i.loc\}$

---

5. Experiments

This section reports the experimental study of the MRLIHT approach. All the experiments are performed on a PC with 3.4 GHz CPU and 16GB RAM.

5.1. Experimental Settings

To evaluate the performance of the proposed MRLIHT, we use the Tossim [28] which is a TinyOS [29] simulator, to simulate an application of indoor exhibition where the size of the visiting area is a 150 m × 150 m rectangular region with the grid. The Visitors (equipped with RFID readers) can move in the visiting area arbitrarily. The RFID tags are deployed on the floor of the visiting area randomly and intensively (liking the deployment shown in Figure 1 introduced in Example 1). Since in our M-RFID model, the RFID tags are fixed deployed in the visiting area, the location of each tag is known and written in its own memory. In the testbed, the type of RFID reader is supposed to be LJYZN-107 with power 915MHz and the radio range is about 10 m. The RFID tags are the labels conforming to the standard of EPC CLASSI G2. The reading rate of tags by readers is generated based on the reader detection model where the parameters are $a_i = 3.6423$ and $b_i = -7.5897$. In addition, we add a random term in a range of $[0, 0.1]$ on the reading rate to simulate the noise in the real application environment.

We adopt the average Euclidean distance between the real locations and estimated locations of RFID readers to measure the accuracy of various location tracking methods. Moreover, we implement

two existing RSS-based indoor location tracking methods, i.e., nearest-neighbor (NN) [24,25] and multilateration (ML) [26] and a newest phase-based mobile reader localization (shorted by PHL) method proposed in [21]. It is notable that in [21], the proposed localization algorithm focuses on determining the location of a mobile RFID reader at a certain axis (e.g., x-axis) while assuming that the position on the other axis (e.g., y-axis) is known and the mobile reader moves along the certain axis. We suppose the assumption limits its application. Thus, in the experiments, we use the phase differences of the tags detected by the mobile reader to replace the RSS, and employ the multilateration to determine the final location of the moving individuals (readers). Finally, we repeat each test 100 times, where in each test we randomly plan a trajectory for each visitor, and the average results are reported to obtain reliable experimental results.

5.2. Selection of Parameters

Recall that the parameters δ_d and δ_s are the distance threshold and size threshold used in tag group generation introduced in Section 4.2.2. Figure 5 reports the distance deviation of MRLIHT-A by varying δ_d and δ_s under the scenarios where 50, 100, 200, 500 tags can be detected by a reader simultaneously. As shown in Figure 5a, with 50 tags can be detected by a reader simultaneously, the lowest distance deviation (3.973 cm) is achieved with $\delta_d = 20$ cm and $\delta_s = 3$. Since the tags are fixed deployment in the monitoring area, we can collect the test readings before the real applications and learn the best δ_d and δ_s based on the test data. In the following experiments, we set the default number of tags that can be detected by a reader simultaneously as 50 until a special illustration.
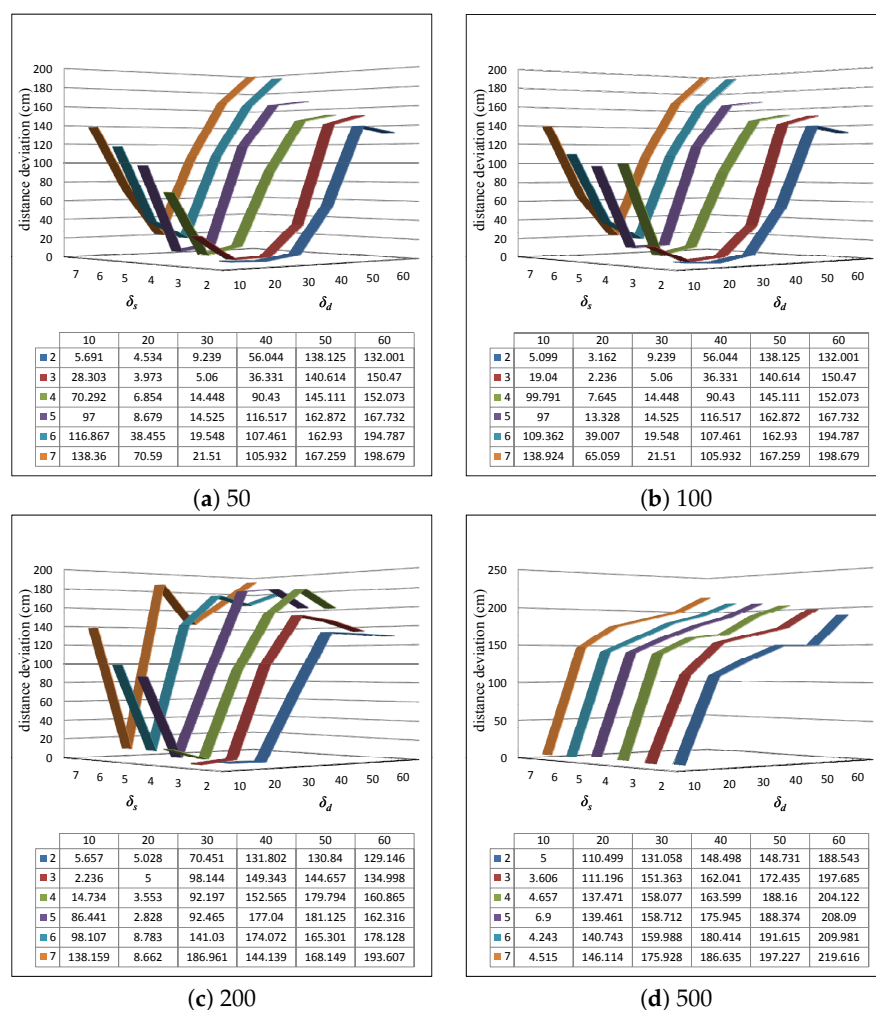

	10	20	30	40	50	60
2	5.691	4.534	9.239	56.044	138.125	132.001
3	28.303	3.973	5.06	36.331	140.614	150.47
4	70.292	6.854	14.448	90.43	145.111	152.073
5	97	8.679	14.525	116.517	162.872	167.732
6	116.867	38.455	19.548	107.461	162.93	194.787
7	138.36	70.59	21.51	105.932	167.259	198.679

(**a**) 50

	10	20	30	40	50	60
2	5.099	3.162	9.239	56.044	138.125	132.001
3	19.04	2.236	5.06	36.331	140.614	150.47
4	99.791	7.645	14.448	90.43	145.111	152.073
5	97	13.328	14.525	116.517	162.872	167.732
6	109.362	39.007	19.548	107.461	162.93	194.787
7	138.924	65.059	21.51	105.932	167.259	198.679

(**b**) 100

	10	20	30	40	50	60
2	5.657	5.028	70.451	131.802	130.84	129.146
3	2.236	5	98.144	149.343	144.657	134.998
4	14.734	3.553	92.197	152.565	179.794	160.865
5	86.441	2.828	92.465	177.04	181.125	162.316
6	98.107	8.783	141.03	174.072	165.301	178.128
7	138.159	8.662	186.961	144.139	168.149	193.607

(**c**) 200

	10	20	30	40	50	60
2	5	110.499	131.058	148.498	148.731	188.543
3	3.606	111.196	151.363	162.041	172.435	197.685
4	4.657	137.471	158.077	163.599	188.16	204.122
5	6.9	139.461	158.712	175.945	188.374	208.09
6	4.243	140.743	159.988	180.414	191.615	209.981
7	4.515	146.114	175.928	186.635	197.227	219.616

(**d**) 500

Figure 5. Varying δ_d and δ_s with 50, 100, 200, 500 tags can be detected by a reader simultaneously.

5.3. Comparison between our Proposed Approaches

In this section, we compare the performance of the proposed MRLIHT based on the exact and approximate PLR generation, respectively, by varying the variance σ of reading rate error ϵ and grid size.

5.3.1. Varying the Variance σ of ϵ

As shown in Figure 6, with an increase of σ, the distance deviations between the estimated locations and ground truths based on both MRLIHT-E and MRLIHT-A decrease. Based on Equation (5), a large σ derives a large RR of a tag to a reader, and thereby derives a large PLR of the reader. Therefore, we can get a more precise location by checking more grids during final location estimation with a larger PLR, while we need to take more time.

(**a**) Distance deviation　　　　　　　　　　　　(**b**) Time cost
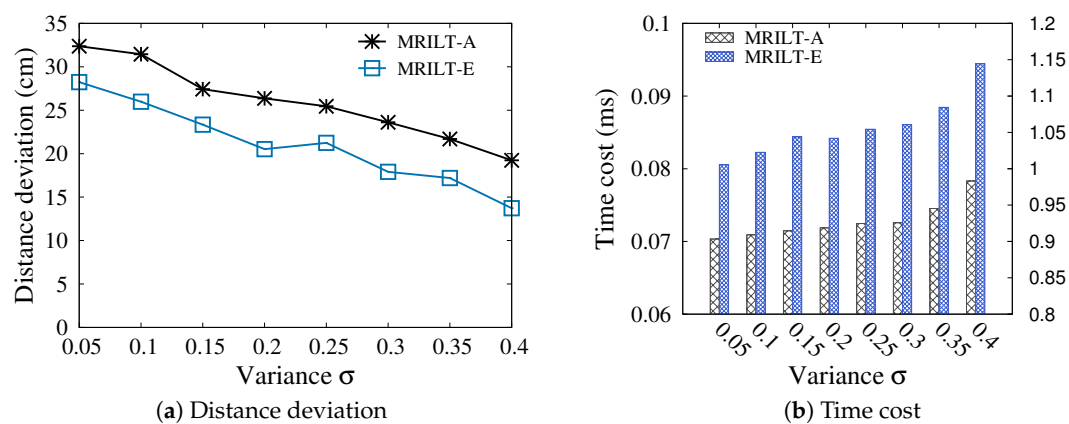
Figure 6. Varying σ with $\delta_d = 20$ cm, $\delta_s = 3$, *grid_size* = 60 cm.

On the other hand, we can observe that the accuracy of location estimation based on MRLIHT-A is slightly higher than that of MRLIHT-E, because in MRLIHT-E, we determine the PLR of a reader by using all tags it detected simultaneously without aggregating those tags into aggregated tags. Moreover, with extensive experiments, the difference between the distance deviation based on MRLIHT-E and the distance deviation based on MRLIHT-A is most 10 cm, which verifies that MRLIHT-A performs well in location tracking. However, the time cost of MRLIHT-A is much lower than that of MRLIHT-E. Since the time cost of MRLIHT-E is one order of magnitude higher than MRLIHT-A (as observed in Figure 6b), we present its time cost by using another ordinate.

5.3.2. Varying the Grid Size

Figure 7 reports the accuracy of location tracking by varying the grid size. Since during location estimation, we consider a grid as a location point, the time cost decrease with the increase of grid size (as shown in Figure 7b) while the accuracy is deteriorated. As shown in Figure 7a, the distance deviations are 4.009 cm and 24.355 cm with grid sizes 10 cm and 60 cm, respectively. We set the default grid size as 60 cm to trade off the positioning accuracy and efficiency.
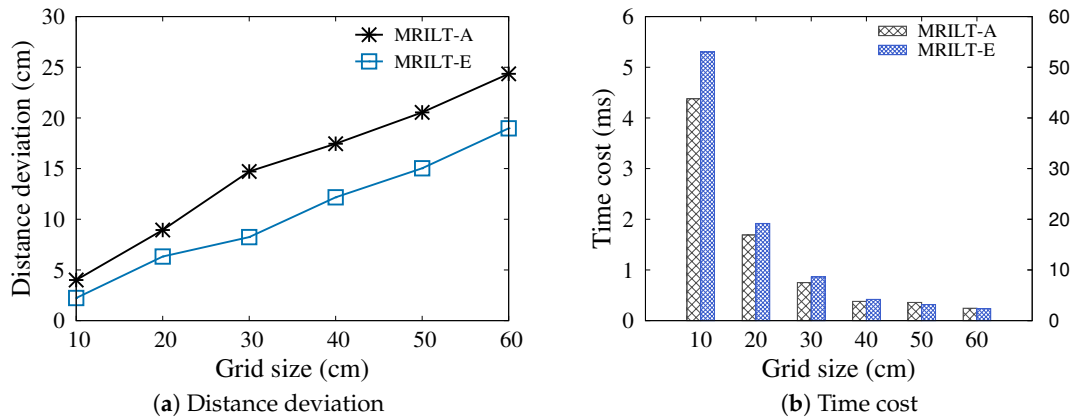
(a) Distance deviation　　　　　　　　　　　**(b)** Time cost

Figure 7. Varying grid size with $\delta_d = 20$ cm, $\delta_s = 3$ and $\sigma = 0.1$.

5.4. Comparison with Existing Methods

In the following experiments, we compare the proposed MRLIHT with existing methods to show that MRLIHT outperforms the state-of-the-art methods.

5.4.1. Varying the Number of Tags Detected by a Reader Simultanesously

Since we estimate the location of moving individuals (readers) based on the readings of tags detected by the reader simultaneously, Figure 8 shows the performance of various methods by varying the number of tags detected by a reader simultaneously. It can be observed from Figure 8a that the lowest distance deviation is achieved by the proposed MRLIHT. The reason is that we consider the uncertainty of the reading rate of a tag by a reader and first extend the candidate locations of a reader into a PLR rather than some certain points. On the other hand, by refining each grid, the positioning accuracy is further improved. Moreover, in NN and ML, the distance between an RFID reader and tags it detected is computed based on the reading rate model whose parameters are learned based on the historical data. During the parameter learning, it inevitably derives some deviations (due to the uncertainty of the reading rate). As a result, the localization algorithms (i.e., NN and ML) without considering this uncertainty derive a large localization deviation. By comparison, in PHL, since the phases are directly collected from reference tags, the distances (between an RFID reader and tags it detected) estimated based on those phases contain relatively small deviations. Therefore, the localization accuracy of PHL is higher than those of NN and ML, but it is lower than our proposed approaches obviously.
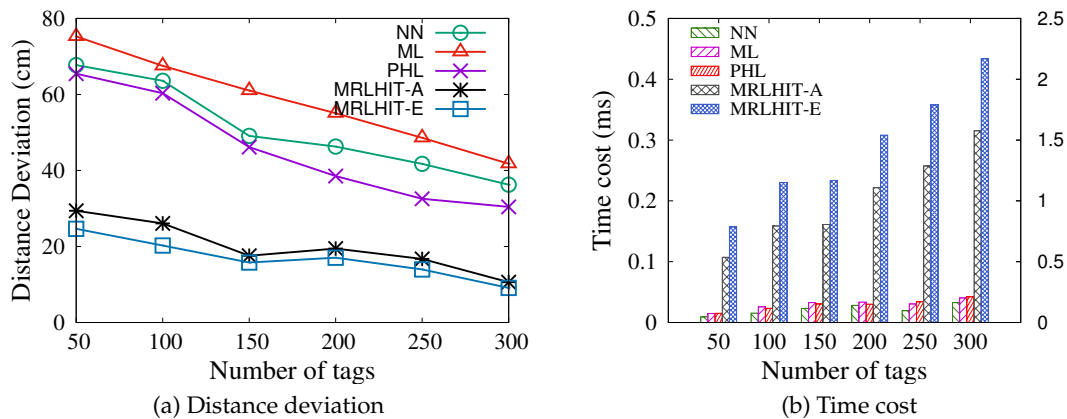

(a) Distance deviation　　　　　　　　　　　(b) Time cost

Figure 8. Varying the number of tags detected simultaneously with $\delta_d = 20$ cm, $\delta_s = 3$, *grid_size* = 60 cm.

As shown in Figure 8b, with the increase of the number of tags, it is not surprising that the time cost rises. The time costs of existing methods NN, ML and PHL (introduced in Section 5.1) are lower than those of MRLIHT-A and MRLIHT-E, but their localization accuracies are also lower. We can observe that the time costs of ML and PHL are close to each other, because both of them estimate the locations of indoor humans based on the multilateration. The main difference between ML and PHL is that the distance between an individual (reader) and a tag is computed based on the RSS and phase difference, respectively. Moreover, we observe that the time costs of the proposed approaches increase approximately linearly, which verifies that they also have good scalability. For example, the time cost of MRLIHT-A is 0.85163 *ms* with 100 tags can be detected by a reader simultaneously, which means we can execute 6300 times of location estimation in a second. On the other hand, we can observe that the time costs of MRLIHT-A are 0.00809 *ms* and 0.2514 *ms* with 50 and 300 tags can be detected simultaneously, respectively. When the tag deployment is intensive, the efficiency of the proposed MRLIHT decreases. Thus in real applications, we should avoid too-intensive tag deployment with a certain accuracy guarantee.

5.4.2. Varying the Number of Readers

Figure 9 reports the evaluation of the scalability in terms of accuracy and efficiency by varying the number of readers. As shown in Figure 9a, the accuracy remains stable with the increase of the count of readers. However, the accuracy of the proposed MRLIHT is higher than the existing methods, obviously. For the time costs, as shown in Figure 9b, all methods increase linearly with the increase of the number of readers. The time costs of MRLIHT-A and MRLIHT-E are 47.5284 ms and 694.6388 ms with 1000 readers, respectively. In other words, we can estimate the locations of 20,000 and 1500 readers in one second based on MRLIHT-A and MRLIHT-E, respectively. Therefore, MRLIHT-A is more suitable for the large-scale monitoring applications without much accuracy sacrifice.
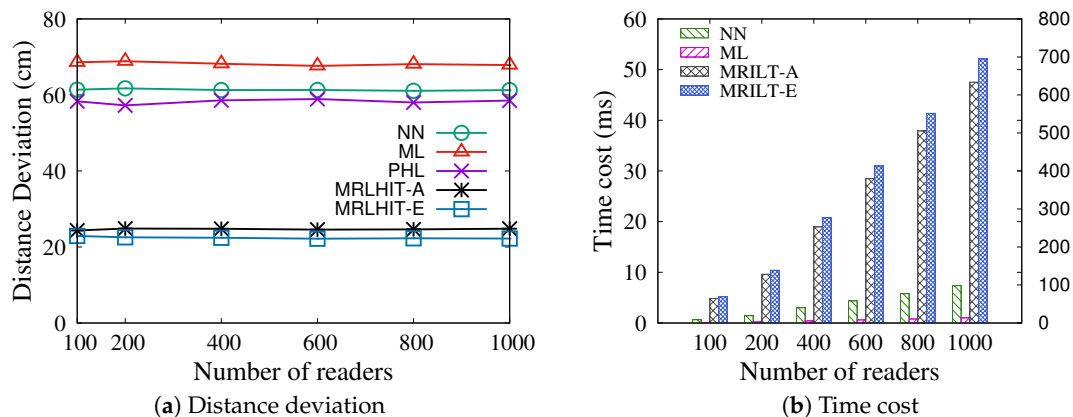

Figure 9. Varying the number of readers with $\delta_d = 20$ cm, $\delta_s = 3$, $grid\_size = 60$ cm.

6. Conclusions

In this paper, we have studied the indoor human tracking problem. Accordingly, we propose a novel M-RFID based localization approach for indoor human tracking, named MRLIHT. In MRLIHT, RFID tags are fixed deployed in the monitoring area intensively, and RFID readers are equipped on the moving objects (i.e., individuals) we targeting to locate. To improve the localization accuracy, we add a random disturbance term which reflects the uncertainty of the readings by an RFID reader on the reading rate. As a result, the response region of an RFID tag to the reader is extended from a circle to a circular, which enriches the candidate positions of the reader. Moreover, in MRLIHT, the individuals can move in the monitoring area arbitrarily without a pre-defined motion model, which is more applicable in the real world. In time cost, since the locations of RFID tags are fixed and can be written in their own memories, the location information of RFID tags (which are used for location tracking)

can be obtained by RFID readers directly. Therefore, the extra queries for tag locations are saved, and thereby the location estimation efficiency is improved. Finally, the extensive experimental results show that the proposed MRLIHT has higher location estimation accuracy than the state-of-the-art methods. Moreover, it is able to accommodate large-scale monitoring applications with good scalability.

Author Contributions: Data curation , formal analysis, investigation, methodology and writing—original draft, Q.M.; Validation, Q.M., M.B. and X.W.; resources, G.L. and B.N.; conceptualization and visualization, X.L. and N.B.; funding acquisition and supervision, Q.M., G.L., M.B. and X.W.; writing—review and editing, Q.M., X.L., M.B. and X.W.; All authors have read and agreed to the published version of the manuscript.

Conflicts of Interest: The authors declare no conflict of interest.

References

1. Finkenzeller, K. *RFID Handbook: Fundamentals and Applications in Contactless Smart Cards, Radio Frequency Identification and Near-Field Communication*; John Wiley & Sons: Manhattan, NY, USA, 2010.
2. Preradovic, S.; Karmakar, N.C. Chipless RFID: Bar code of the future. *IEEE Microw. Mag.* **2010**, *11*, 87–97.
3. Nikitin, P.; Martinez, R. Method, System and Apparatus for Locating RFID Tags. U.S. Patent US20200034583A1, 30 January 2020.
4. Yan, D.; Zhao, Z.; Ng, W.; Leveraging read rates of passive RFID tags for real-time indoor location tracking. In Proceedings of the 21st ACM International Conference on Information and Knowledge Management, Maui, HI, USA, 29 October–2 Novembe, 2012; pp. 375–384.
5. Yang, L.; Yang, Y.; Mgaya, G.B.; Zhang, B.; Chen, L.; Liu, B. Novel Fast Networking Approaches Mining Underlying Structures From Investment Big Data. *IEEE Trans. Syst. Man Cybern. Syst. (Early Access)* **2020**. [CrossRef]
6. Ni, L.M.; Liu, Y.; Lau, Y.C.; Patil, A.P. LANDMARC: Indoor location sensing using active RFID. In Proceedings of the First IEEE International Conference on Pervasive Computing and Communications, 2003. (PerCom 2003), Fort Worth, TX, USA, 26–26 March 2003; pp. 407–415.
7. Bahl, P.; Padmanabhan, V.N. RADAR: An in-building RF-based user location and tracking system. In Proceedings of the IEEE INFOCOM 2000. Conference on Computer Communications. Nineteenth Annual Joint Conference of the IEEE Computer and Communications Societies, Tel Aviv, Israel, 26–30 March 2000; pp. 775–784.
8. Öktem, R.; Aydin, E. An RFID based indoor tracking method for navigating visually impaired people. *Turk. J. Electr. Eng. Comput. Sci.* **2010**, *18*, 185–198.
9. Wang, J.; Katabi, D. Dude, where's my card? RFID positioning that works with multipath and non-line of sight. In Proceedings of the ACM SIGCOMM 2013 Conference on SIGCOMM, Hong Kong, China, 12–16 August 2013; pp. 51–62.
10. Liu, T.; Yang, L.; Lin, Q. Anchor-free backscatter positioning for RFID tags with high accuracy. In Proceedings of the IEEE INFOCOM 2014—IEEE Conference on Computer Communications, Toronto, ON, Canada, 27 April–2 May 2014; pp. 379–387.
11. Zhou, M.; Tang, Y.; Tian, Z.; Xie, L.B.; Nie, W. Robust neighborhood graphing for semi-supervised indoor localization with light-loaded location fingerprinting. *IEEE Internet Things J.* **2018**, *5*, 3378–3387. [CrossRef]
12. Chen, H.; Ku, W.S.; Wang, H.; Sun, M. Leveraging spatio-temporal redundancy for RFID data cleansing. In Proceedings of the 2010 ACM SIGMOD International Conference on Management of Data, Indianapolis, IN, USA, 6–11 June 2010; pp. 51–62.
13. Zhao, Z.; Ng, W. A model-based approach for RFID data stream cleansing. In Proceedings of the 21st ACM International Conference on Information and Knowledge Management, Maui, HI, USA, 29 October–2 November 2012; pp. 862–871.
14. Shangguan, L.; Li, Z.; Yang, Z.; Li, M.; Liu, Y.H. OTrack: Towards order tracking for tags in mobile RFID systems. *TPDS* **2013**, *25*, 2114–2125.

15. Yang, L.; Chen, Y.; Li, X.Y.; Xiao, C.W., Li, M.; Liu, Y.H. Tagoram: Real-time tracking of mobile RFID tags to high precision using COTS devices. In Proceedings of the 20th Annual International Conference on Mobile Computing and Networking, Maui, HI, USA, 7–11 September 2014; pp. 237–248.

16. Shangguan, L.; Shangguan, K. The design and implementation of a mobile RFID tag sorting robot. In Proceedings of the 14th Annual International Conference on Mobile Systems, Applications, and Services, Suntec, Singapore, 26–30 June 2016; pp. 31–42.

17. Gu, Y.; Guo, N.; Yu, G. Study on Processing Probabilistic RFID Spatial Range Query Based on Mobile Readers. *Chin. J. Comput.* **2009**, *32*, 2052–2065.

18. Tran, T.; Sutton, C.; Cocci, R.; Nie, Y.; Diao, Y.; Shenoy, P. Probabilistic inference over RFID streams in mobile environments. In Proceedings of the 2009 IEEE 25th International Conference on Data Engineering, Shanghai, China, 29 March–2 April 2009; pp. 1096–1107.

19. Bapat, T.A.; Candan, K.S.;Cherukuri, V.S.; Sundaram, H. AURA: Enabling attribute-based spatial search in RFID rich environments. In Proceedings of the 2009 IEEE 25th International Conference on Data Engineering, Shanghai, China, 29 March–2 April 2009; pp. 1211–1214.

20. Bapat, T.A.; Candan, K.S.; Cherukuri, V.S.; Sundaram. H. Information-gradient based decentralized data management over RFID tag clouds. In Proceedings of the 2009 Tenth International Conference on Mobile Data Management: Systems, Services and Middleware, Taipei, Taiwan, 18–21 May 2009; pp. 72–81.

21. Motroni, A.; Buffi, A.; Nepa, P. Localization of a mobile device equipped with an RFID reader. In Proceedings of the 2017 IEEE International Conference on RFID Technology & Application (RFID-TA), Warsaw, Poland, 20–22 September, 2017; pp. 74–79.

22. Shangguan, L.; Yang, Z.; Liu, A.X.; Zhou, Z.M.; Liu, Y.H. Relative Localization of RFID Tags using Spatial-Temporal Phase Profiling. In Procreedings of the NSDI '15, Santa Clara, CA, USA, 6–7 July 2015; pp. 251–263.

23. Lai, J.; Luo, C.; Wu, J.; Li, J.; Wang, J.; Chen, J.; Feng, G.; Song, H. TagSort: Accurate Relative Localization Exploring RFID Phase Spectrum Matching for Internet of Things. *IEEE Internet Things J.* **2020**, *5*, 389–399. [CrossRef]

24. Li, D.; Zhang, B.; Li, C. A feature-scaling-based *k*-nearest neighbor algorithm for indoor positioning systems. *IEEE Internet Things J.* **2015**, *3*, 590–597. [CrossRef]

25. Morales, J.; Akopian, D.; Agaian, S. Mitigating anomalous measurements for indoor wireless local area network positioning. *IET Radar Sona Navig.* **2016**, *10*, 1220–1227. [CrossRef]

26. Zhou, J.; Shi, J. RFID localization algorithms and applications—A review. *J. Intell. Manuf.* **2009**, *20*, 695–707. [CrossRef]

27. Yang, W.B.; Xing, P.K.; Liu, Y.H. A Positioning Method for WSN Based on Self-Adapted RSSI Distance Model. *Chin. J. Sens. Actuators* **2015**, *28*, 137–141.

28. Levis, P.; Lee, N.; Welsh, M.; Culler, D. TOSSIM: Accurate and scalable simulation of entire TinyOS applications. In Proceedings of the 1st International Conference on Embedded Networked Sensor Systems, Los Angeles, CA, USA, 5–7 November 2003; pp. 126–137.

29. Chandanashree, V.C.; Bhat, U.P.; Kanade, P.; Arjun, K.M.; Gagandeep, J.; Hegde, R.M. Tinyos based WSN design for monitoring of cold storage warehouses using internet of things. In Proceedings of the 2017 International conference on Microelectronic Devices, Circuits and Systems (ICMDCS), Vellore, India, 10–12 August 2017; pp 1–6.